

# Journal of Composite Materials

<http://jcm.sagepub.com/>

---

## Organoclay Effect on Mechanical Responses of Glass/Epoxy Nanocomposites

Jia-Lin Tsai and Ming-Daw Wu

*Journal of Composite Materials* 2007 41: 2513

DOI: 10.1177/0021998307076491

The online version of this article can be found at:

<http://jcm.sagepub.com/content/41/20/2513>

---

Published by:



<http://www.sagepublications.com>

On behalf of:



American Society for Composites

Additional services and information for *Journal of Composite Materials* can be found at:

**Email Alerts:** <http://jcm.sagepub.com/cgi/alerts>

**Subscriptions:** <http://jcm.sagepub.com/subscriptions>

**Reprints:** <http://www.sagepub.com/journalsReprints.nav>

**Permissions:** <http://www.sagepub.com/journalsPermissions.nav>

**Citations:** <http://jcm.sagepub.com/content/41/20/2513.refs.html>

>> [Version of Record](#) - Sep 27, 2007

[What is This?](#)

# Organoclay Effect on Mechanical Responses of Glass/Epoxy Nanocomposites

JIA-LIN TSAI\* AND MING-DAW WU

*Department of Mechanical Engineering  
National Chiao Tung University, Hsinchu, Taiwan 300*

**ABSTRACT:** This research aims to perform a symmetric investigation regarding the organoclay effect on the mechanical behaviors of glass/epoxy nanocomposites. Tensile, flexural, as well as interlaminar fracture toughness are of concern in this study. To demonstrate the organoclay effect, three different loadings, 2.5, 5, and 7.5 wt% of organoclay were dispersed in the epoxy resin using a mechanical mixer followed by sonication. The corresponding glass/epoxy nanocomposites were prepared by inserting the organoclay epoxy mixture into the dry glass fiber through a vacuum hand lay-up process. Tensile tests revealed that longitudinal tensile strength decreases as organoclay loading increases; on the other hand, transverse tensile strength increases with the increase of the organoclay. Furthermore, scanning electron microscopy observation on the transverse failure specimens indicates that the enhanced mechanism is due to the improved interfacial bonding between the fibers and the surrounding matrix modified by organoclay. The increasing tendency was also found in the transverse flexural strength of the nanocomposites. However, mode I fracture tests indicated that with the increase of the organoclay, the corresponding fracture toughness of the nanocomposites decreases appreciably. For the quasi-isotropic glass/epoxy laminates, since the failure is dominated by fiber rupture, the strength is not influenced significantly by the organoclay.

**KEY WORDS:** organoclay, glass/epoxy nanocomposites, tensile strength, flexural properties, interlaminar fracture toughness.

## INTRODUCTION

HAVING CHARACTERISTICS OF superior mechanical behaviors and higher aspect ratio, the nano-materials are considered a supreme reinforcement for improving matrix properties [1,2]. Polymer reinforced with organoclay platelets is one particular class of nanocomposites and has attracted considerable attention since Toyota researchers successfully enhanced the mechanical properties of nylon-6 a decade ago [3,4]. The organoclay platelet is an ultra thin (1 nm) silicate film with lateral dimensions up to 1 $\mu$ m. Through the ion exchange process, the sodium ions attracted on the surfaces of the

---

\*Author to whom correspondence should be addressed. E-mail: [jjalin@mail.nctu.edu.tw](mailto:jjalin@mail.nctu.edu.tw)  
Figures 9, 16 and 17 appear in color online: <http://jcm.sagepub.com>

platelets were replaced with organic cations which cannot only improve the interfacial adhesion between the polymer and the platelet but also facilitate the exfoliation of the organoclay. After an appropriate fabrication process, such as melt compounding [5], *in situ* polymerization [6,7] and solution method [8], the aggregated platelets can be exfoliated and dispersed uniformly in the polymer. Depending on the degree of exfoliation, three categories of nanocomposites, i.e., tactoid, intercalated and exfoliated, could be produced [9]. Experimental observations show that the stiffness of nanocomposites can be enhanced appreciably if the platelets are well dispersed and exfoliated in the nanocomposites [5,10].

Although the mechanical behaviors of nanocomposites can be increased by organoclay, as compared to the conventional fiber composites, the enhancement is still limited. To be viable for structural applications, the hybrid fiber/organoclay nanocomposites, combining the characteristics of the long fiber composites and the organoclay nanocomposites, were then synthesized. Haque et al. [11] fabricated the glass/epoxy composites and glass/epoxy nanocomposites with low loading of organoclay. They point out that dispersion of 1 wt% organoclay could improve the interlaminar shear strength of glass/epoxy nanocomposites up to 44%. Similar tendency on the flexure properties of the laminates with organoclay was also observed by Kornmann et al. [12]. Chowdhury et al. [13] studied the flexural and thermo-mechanical properties of woven carbon carbon/nanoclay epoxy laminates and posit that the samples containing 2 wt% organoclay loading possess the maximum flexural strength and modulus as well as the highest  $T_g$  value. Miyagawa et al. [14] investigated the organoclay effect on flexural properties and interlaminar shear strength (ILSS) of bio-based epoxy carbon fiber composites. It was found that the flexural strength and the modulus are not influenced substantially by the organoclay. In addition, little improvement on the ILSS was observed on the 5 wt% organoclay samples. Vlasveld et al. [15] conducted a single fiber fragmentation test to evaluate the fiber-matrix interfacial bonding properties of the glass fiber reinforced polyimide-6 silicate nanocomposites. It was revealed that interfacial bonding decreases with the inclusion of silicate into the matrix materials, which deviates from earlier investigations by other researchers [11–13]. This discrepancy could be due to the processing effect resulting in changes of the microstructures of the nanocomposites. So far, the information related to the effect of organoclay on the mechanical responses of fiber/epoxy nanocomposites is still lacking.

In this study, systematic experiments were carried out to understand the organoclay effect on the tensile, flexural, and interlaminar fracture behaviors of glass fiber reinforced nanocomposites. The associated failure mechanisms were determined by scanning electron microscopy (SEM) observations on the failure surfaces. Moreover, the quasi-isotropic laminates with different organoclay loadings were fabricated, and the corresponding tensile strength was measured from the tensile tests. Experimental results were compared with those obtained from conventional composites.

## MATERIAL PREPARATIONS

To investigate the organoclay effect on tensile, flexural, and fracture properties of glass/epoxy nanocomposites, the laminate plates with various organoclay loadings were prepared. Subsequently, based on different experimental purposes, the corresponding specimens were fabricated.

### Preparation of Glass/Epoxy/Organoclay Nanocomposites

The epoxy resin used in this study is diglycidyl ether of bisphenol A (DGEBA, EPON828 with an epoxy equivalent weight of 187) supplied by Resolution Performance Products. The curing agent is polyoxypropylenediamine (Jeffamine D-230 with a molecular weight of 230) provided by Huntsman Corporation. The clay used for the synthesis of nanocomposites is organoclay (Nanomer I.30E) obtained from Nanocor, Inc. It is basically an octadecyl-ammonium ion surface modified montmorillonite mineral designed to be easily dispersed into amine-cured epoxy resin and form nanocomposites as well [16]. Before the fabrication process, the organoclay clay was dried in a vacuum oven for 6 h at 90°C in order to remove moisture and then blended with EPON828 at 80°C for 4 h using a mechanical stirrer. The mixture was then sonicated using a sonicator with a cooling system around the sample container until the compounds became transparent. It should be noted that sonication is an ultrasonic liquid processing. In the liquid compound, microscopic bubbles form momentarily and then implode by means of ultrasonic vibration. The collapse of thousands of bubbles can cause powerful shock waves to radiate throughout the sample resulting in clay platelet separation. The epoxy/organoclay mixture was degassed at room temperature in a vacuum oven for 10 min and mixed with a curing agent (32 wt% of EPON828). The mechanical stirrer was again utilized to blend the final mixture at room temperature for 10 min. It is noted that from the X-ray diffraction (XRD) measurements and transmission electron microscopy (TEM) observations, the samples prepared in this manner were characterized as intercalated nanocomposites [17].

Vacuum-assisted hand lay-up procedures were adopted for preparing the glass fiber/epoxy nanocomposites. The mixture of organoclay/epoxy together with the curing agent was poured onto one dry unidirectional glass fiber layer (provided by Vectorply®, E-LR0908-14 unidirectional E-glass fiber). The resin was incorporated into the dry fiber using a hand roller. Then another ply of dry fiber was stacked on it. This process continued repeatedly until the desired layers of glass fiber nanocomposites were developed. The fiber stack was sandwiched between two steel plates with porous Teflon fabric on the surface and then sealed within a vacuum bag. The whole laminates were cured in a hot press at the suggested temperature profile with vacuum conditions. The vacuum is essential for forming nanocomposites since it can facilitate the removal of tiny bubbles trapped in the nanocomposites during the process.

### Fabrication of Nanocomposite Specimens

There were several categories of specimens prepared for investigating the organoclay effect on the nanocomposite behaviors such as the tensile, flexure, and fracture properties. Unidirectional [0]<sub>5</sub> and [90]<sub>5</sub> laminates were prepared for evaluating the tensile strength and modulus of the nanocomposites in longitudinally and transversely, respectively. In addition, the in-plane shear strength of the nanocomposites was determined from the tensile tests on off-axis [10]<sub>5</sub> specimens and [±45]<sub>5</sub> laminates. With regard to the flexure properties of the nanocomposites, three-point bending tests were conducted on the [0]<sub>5</sub> and [90]<sub>5</sub> specimens, respectively. Interlaminar delamination fracture toughness of the nanocomposites was evaluated using double cantilever beam (DCB) specimens. It is noted that the forgoing specimens are designed for characterizing the fundamental mechanical

properties of unidirectional nanocomposites associated with various organoclay loadings. In order to understand the organoclay effect on the nanocomposite laminates, two quasi-isotropic nanocomposites,  $[0/\pm 45/90]_s$  and  $[0/\pm 60]_s$ , were prepared accordingly. The coupon specimens cut from the laminate plates using a diamond saw with appropriate orientation were prepared for tensile testing.

## MECHANICAL PROPERTY CHARACTERIZATION

In order to understand the organoclay effect on the mechanical properties of the glass fiber reinforced nanocomposites, a series of experimental tasks were carried out, and the associated results were compared to the conventional composites containing no organoclay.

### Tensile Tests

To determine the tensile behavior, coupon specimens (200 mm long, 18 mm wide and 1.45 mm in thickness) obtained from five-ply unidirectional nanocomposites were employed for tension tests. Because both ends of the tensile specimens were attached to the end tabs, the actual gage length is 100 mm. Tensile tests were conducted on the hydraulic MTS machine using the stroke control mode at a strain rate of  $10^{-4}$ /s. During the tests, the strain histories were measured from the strain gauges adhered back-to-back on the central section of the specimens; at the same time, the corresponding loadings were obtained from the load cell mounted on the loading fixture. Both signals were recorded concurrently using a personal computer with the Labview program.

### *[0]<sub>5</sub> TENSION*

The tensile strength and Young's modulus of the nanocomposites with different organoclay loadings were evaluated from the peak values and the initial slope (0.1% strain) of the stress-strain curves of the  $[0]_5$  specimens, respectively. Since they are fiber-dominated properties, the stress-strain curve is linear, and the sudden failure occurs when the ultimate strength is achieved. Figures 1 and 2 illustrate Young's modulus and longitudinal tensile strength of the nanocomposites with respect to different organoclay loadings. At least five specimens were tested for each case. It was found that Young's modulus is not affected significantly by the organoclay; however, the failure stresses decline as the organoclay loading increases. In general, the tensile strength is dominated by fiber property which should not be influenced appreciably by the matrix. It is noted that the fibers adopted for the study are stitched together by the woven threads which may cause the fibers to be wavy in the nanocomposites. When the samples with the wavy fibers are tested in the fiber direction, the failure mechanism may not be dominated by fiber breakages. During the experiments, a sudden fiber broom failure associated with popping sounds caused by fiber bundle separation was observed on the  $[0]_5$  specimens instead of fiber rupture. In addition, when the epoxy matrix is modified with the organoclay, the mechanical response may become brittle such that fracture toughness decreases [17]. As a result, the effect of wavy fibers in conjunction with the brittle behaviors of the matrix should be responsible for the decrease in tensile strength.

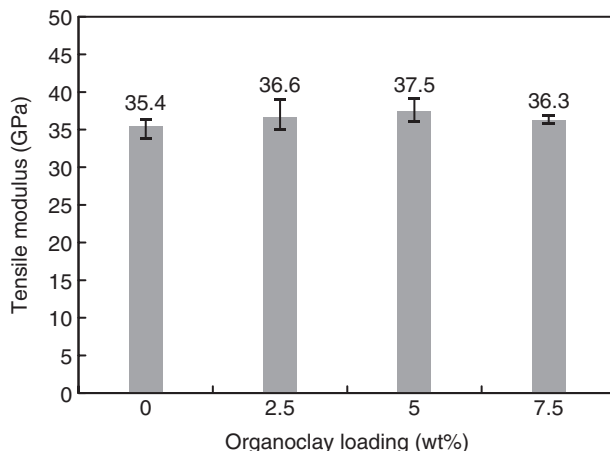


**Figure 1.** Longitudinal tensile modulus of glass fiber/epoxy nanocomposites with various organoclay loadings.

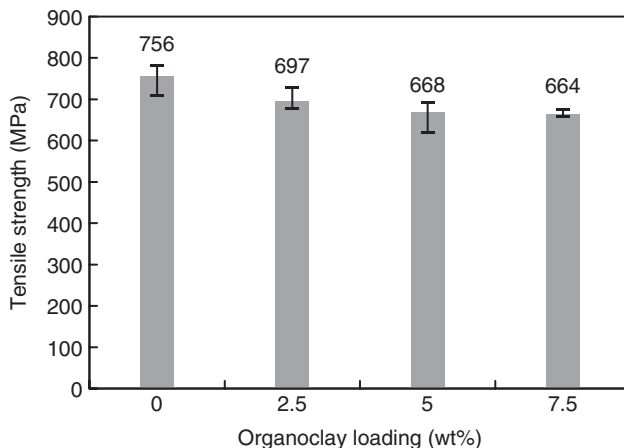


**Figure 2.** Longitudinal tensile strength of glass fiber/epoxy nanocomposites with various organoclay loadings.

*[90]<sub>5</sub> TENSION*

Transverse tensile modulus and strength were measured from the tensile tests on [90]<sub>5</sub> specimens. In contrast to the tensile strength discussed earlier, both transverse tensile modulus and strength exhibit increasing behaviors with the increment of organoclay loading, and the results are illustrated in Figures 3 and 4, respectively. For the transverse tensile modulus, the improvement could be attributed to the stiffened behavior of the matrix modified by organoclay [10,17]. In order to further understand the enhancing mechanism on tensile strength, the failure surfaces of the samples were observed using SEM. For comparison purposes, the nanocomposites with 5 wt% organoclay as well as that with no organoclay included were taken into consideration, and the respective micrographics are shown in Figure 5. It was found that for the nanocomposites, the fibers

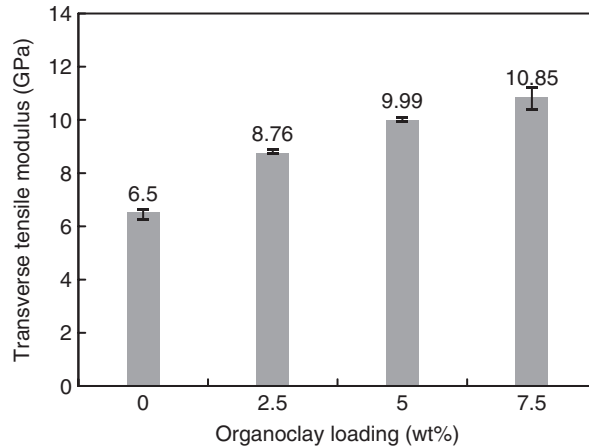


**Figure 3.** Transverse tensile modulus of glass fiber/epoxy nanocomposites with various organoclay loadings.

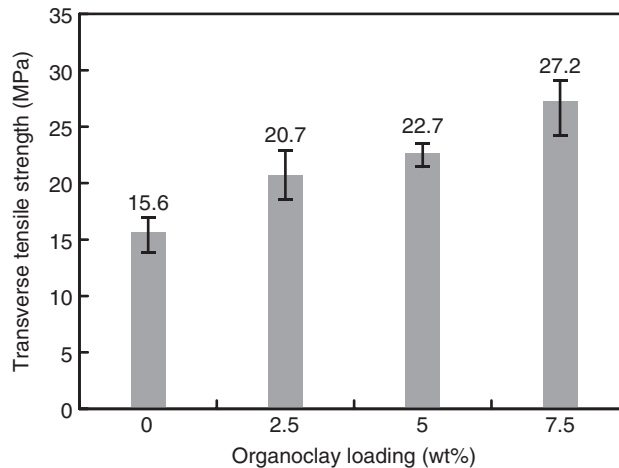


**Figure 4.** Transverse tensile strength of glass fiber/epoxy nanocomposites with various organoclay loadings.

still surrounded and adhered to the matrix; consequently, matrix cracking is the primary failure mechanism. On the other hand, for the conventional composites, the failure surfaces of the fibers are featureless and smooth, which indicate that interfacial debonding is the main failure mechanism. According to SEM observations, it appears that the nanocomposites modified by the organoclay possess better interfacial bonding than the conventional ones. As a result, the increasing behavior of the transverse tensile strength in the nanocomposites could be attributed to the improved interfacial strength provided by the organoclay. The organoclay effect on the interfacial bonding of glass fiber nanocomposites is currently under investigation using molecular mechanics analysis.

#### [10]<sub>5</sub> TENSION

In view of the forgoing, it seems that the interfacial adhesion between the glass fibers and the surrounding matrix can be improved effectively by organoclay. This phenomenon

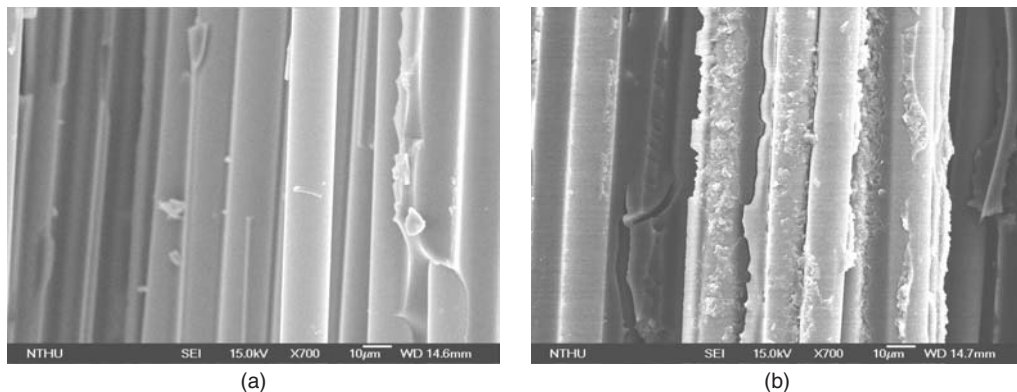


**Figure 5.** SEM micrographics of glass fiber/epoxy nanocomposites samples: (a) pure epoxy; (b) 5 wt% organoclay.

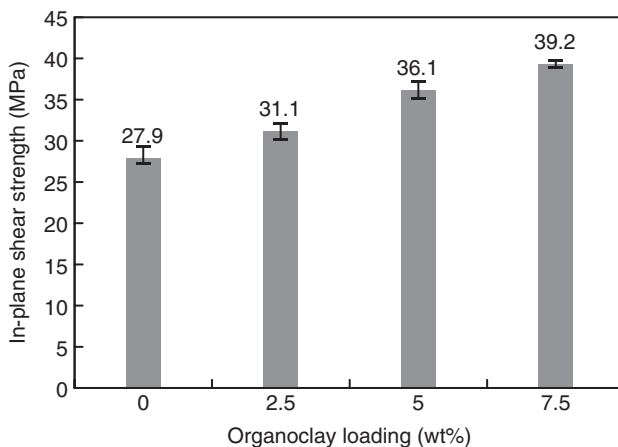


**Figure 6.** In-plane shear strength of glass fiber/epoxy nanocomposites obtained from 10° off-axis specimens.

implies that the in-plane shear strength of nanocomposites which is dominated by interfacial properties could also be enhanced appropriately. To validate the above statement, the in-plane shear strength of fiber reinforced nanocomposites was measured from off-axis 10° specimens and the [±45]<sub>s</sub> laminates [18]. The 10° specimens are introduced in this section, and the [±45]<sub>s</sub> laminates are presented in the next section. It is noted that in the 10° specimens, the tensile normal stress is always accompanied with the in-plane shear stress on the failure plane resulting in that the in-plane shear strength measured from 10° specimens is relatively low compared to that obtained from [±45]<sub>s</sub>; thus, the results measured from 10° specimens are considered as the lower bound solution. The in-plane shear strength obtained from the off-axis 10° specimens is plotted in Figure 6 with respect to different organoclay loadings. It is revealed that in-plane shear strength increases as the organoclay loading rises. SEM micrographics on the failure surfaces, as shown in Figure 7, also indicate that the interfacial bonding in the nanocomposites is superior to that in the conventional composites. Therefore, in addition to the transverse



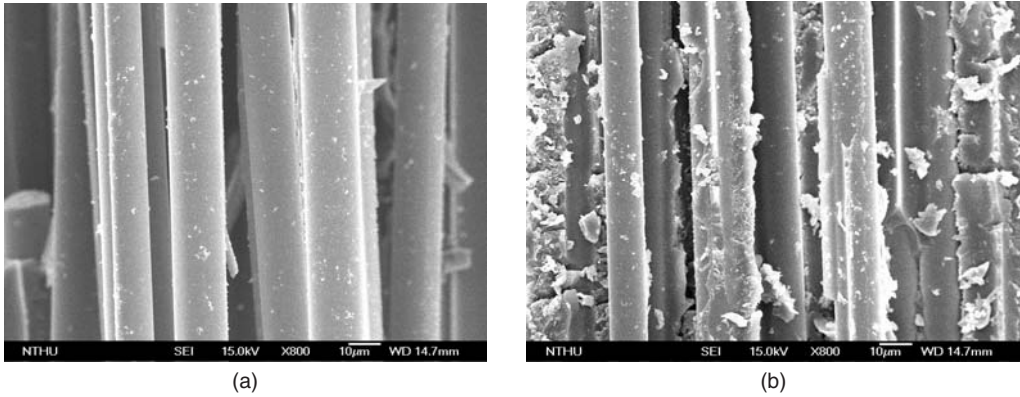


**Figure 7.** SEM micrographics of  $10^\circ$  off-axis glass fiber/epoxy nanocomposite specimens: (a) pure epoxy; (b) 5 wt% organoclay.

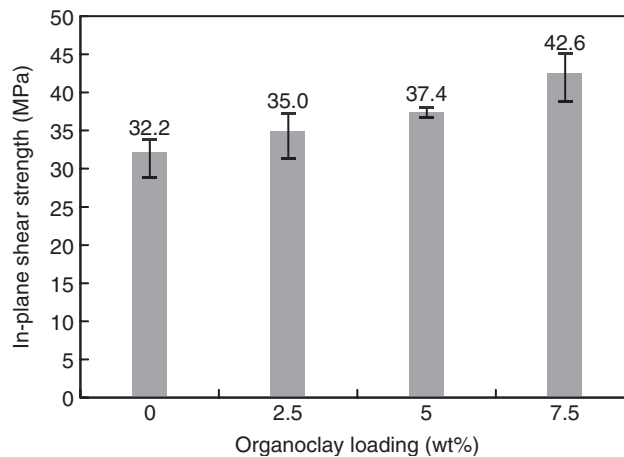


**Figure 8.** In-plane shear strength of glass fiber/epoxy nanocomposites obtained from  $[\pm 45]_s$  laminates.

responses, the in-plane properties of the nanocomposites can be enhanced appropriately by the dispersion of the organoclay in the epoxy matrix.

#### $[\pm 45]_s$ TENSION

The in-plane shear strength of the nanocomposites was also characterized from tensile tests on  $[\pm 45]_s$  laminate. The experimental results are shown in Figure 8. As compared to the values determined from the off-axis  $[10]_5$  specimens, the in-plane shear strength measured from the  $[\pm 45]_s$  laminate is relatively higher. This is because of the constraint effect caused by the adjacent plies; thus, the associated measurement is regarded as the upper bound solution. Moreover, it is found that the in-plane shear strength obtained from  $[\pm 45]_s$  laminate increases as the organoclay contents increase, which is basically consistent with the results from  $[10]_5$  specimens. The failure specimens for the nanocomposites containing 5 wt% organoclay loading as well as the conventional ones

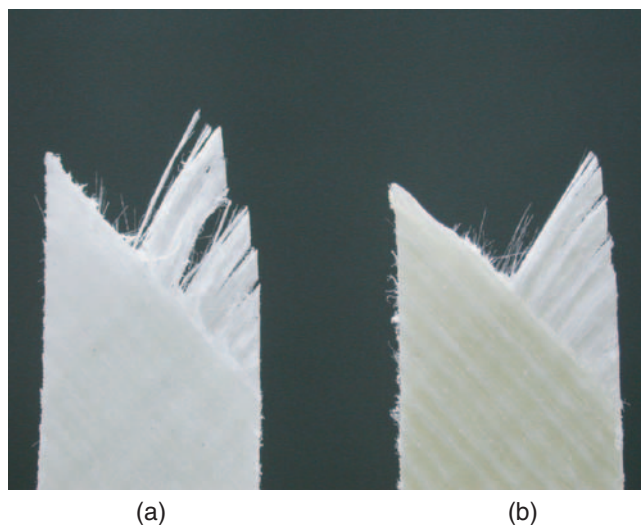


**Figure 9.** Failure specimens of  $[\pm 45]_s$  glass fiber/epoxy nanocomposites: (a) pure epoxy; (b) 5 wt% organoclay.

are shown in Figure 9, respectively, which suggests that for the  $[\pm 45]_s$  laminates, there is no obvious fiber rupture observed, and, as a result, matrix failure is the primary failure mechanism.

### Three-Point Bending Flexure Tests

The effect of organoclay on the flexural properties of the glass fiber reinforced nanocomposites was determined from the three-point bending test in accordance with ASTM standard D790 [19]. During the tests, the crosshead is under stroke control, and the corresponding speed is set at 0.07 mm/min. The flexural strength of the specimens is calculated from the formulation:

$$S = \frac{3PL}{2bd^2}. \quad (1)$$

where  $P$  is the failure load,  $L$  is the support span, and  $b$  and  $d$  represent the width and thickness of the specimens, respectively.

#### $[0]_5$ FLEXURE TESTS

Longitudinal flexural strengths of the nanocomposites, as well as the conventional composites, are shown in Figure 10. No significant improvement on flexural strength was observed in the nanocomposites. This response is normal because the longitudinal flexural properties are controlled by the fiber properties.

#### $[90]_5$ FLEXURE TESTS

To evaluate the transverse flexural strengths of the nanocomposites, the three-point bending tests were carried out on the  $[90]_5$  specimens. The experimental results in terms of

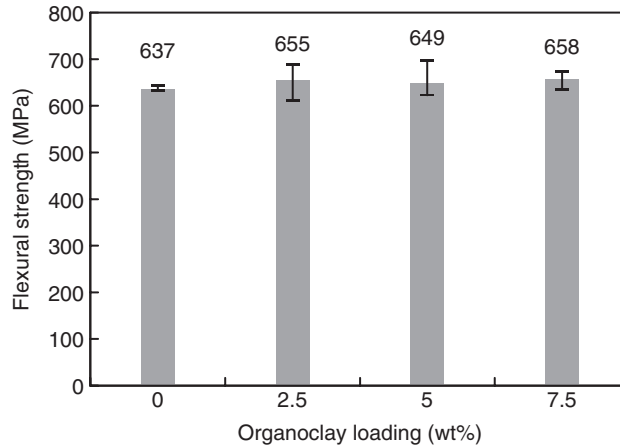


**Figure 10.** Longitudinal flexure strength of glass fiber/epoxy nanocomposites with various organoclay loadings.

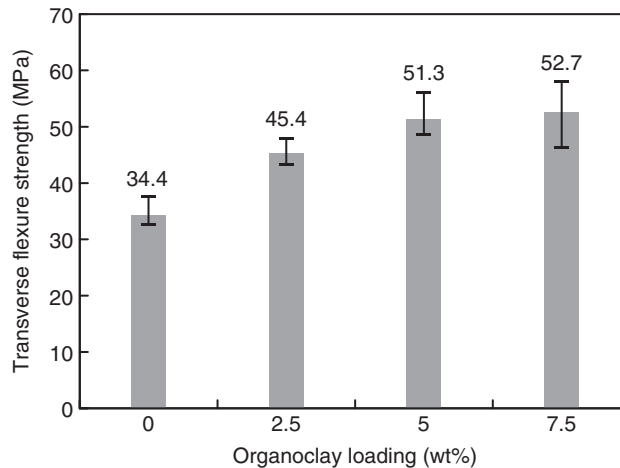


**Figure 11.** Transverse flexure strength of glass fiber/epoxy nanocomposites with various organoclay loadings.

organoclay contents are shown in Figure 11. It appears that as the organoclay increases, the transverse flexural strength increases accordingly. Since the transverse flexural behaviors are governed by the matrix properties, based on previous discussions, it is not surprising that the failure strength should be enhanced with the increase of organoclay loadings.

### Mode I Fracture Test

Since interlaminar delamination frequently occurs in fiber-reinforced polymeric composite, it is necessary to understand the role of organoclay on interlaminar fracture

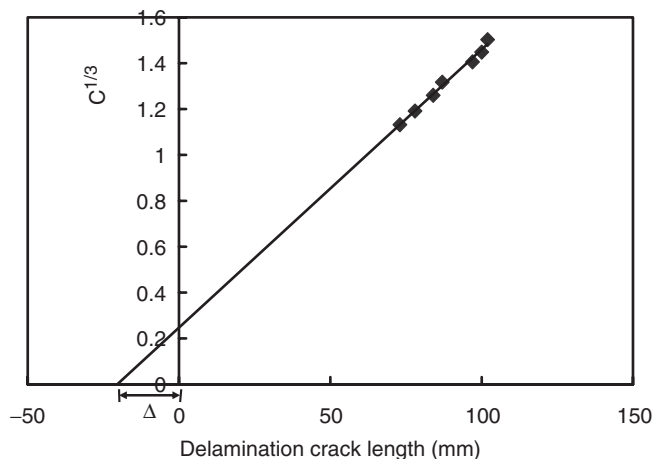


**Figure 12.** Determination of the parameter  $\Delta$  in the modified beam theory.

behaviors. Interlaminar fracture toughness was measured from the DCB specimens which are 12-ply unidirectional laminates with a porous film inserted in the mid-plane during the lay-up process for creating the pre-crack. The dimensions of the specimen are 230 mm long, 20 mm wide, and 3.3 mm thick. Symmetric loadings applied in opposite directions were transferred into the cracked end of the specimens through a pair of hinges bonded on the specimen surfaces resulting in the mode I crack extension. During testing, the initial crosshead rate is 3 mm/min and then reduced to 0.5 mm/min before the onset of delamination extension. All specimen preparations and experimental procedures were performed based on ASTM standard D5528-01 [20]. Fracture toughness was calculated using the modified beam theory [21]:

$$G_{IC} = \frac{3P\delta}{2B(a + \Delta)} \quad (2)$$

where  $P$  is the load when cracks begin to propagate, and  $\delta$  is the displacement associated with the load  $P$ ;  $B$  is the width, and  $a$  is the initial crack length of the specimen. In conventional beam theory, fracture toughness was calculated based on the assumption that the specimen is clamped at the delamination crack front. However, in reality, the DCB specimen is not a perfectly built-in cantilever but exhibits rotation and deformation around the crack tip. To compensate the deformation and rotation effect, the beam theory was modified with a slightly longer crack length  $a + \Delta$ , where  $\Delta$  can be evaluated experimentally from the plot of the cube root of compliance with respect to the crack length as shown in Figure 12. The interlaminar mode I fracture toughness of the nanocomposites calculated from the modified beam theory are plotted vs. the organoclay loading in Figure 13. In contrast to in-plane shear strength and transverse tensile strength, the interlaminar fracture toughness of the nanocomposites decreases as the organoclay loading increases. For the matrix modified with the organoclay, the corresponding mechanical properties become brittle so that the plastic zone around the crack tip is small, allowing the crack to extend easily. As a result, the presence of

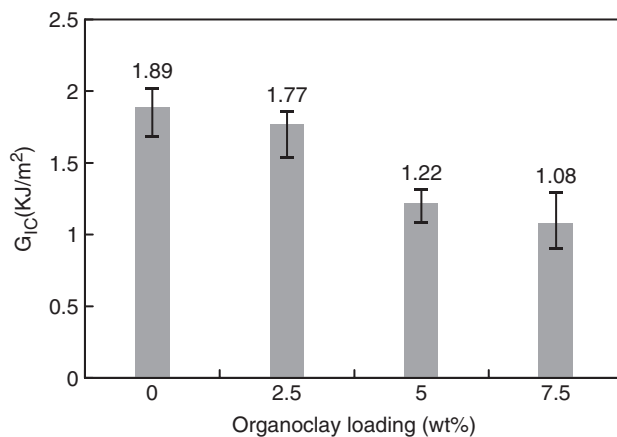


**Figure 13.** Interlaminar Mode I fracture toughness of glass fiber/epoxy nanocomposites with various organoclay loadings.

organoclay has a negative effect on the interlaminar fracture toughness of the fiber-reinforced nanocomposites.

### Quasi-isotropic Laminates

In addition to the unidirectional glass/epoxy nanocomposites, the influence of organoclay on the mechanical responses of quasi-isotropic laminates was investigated. Two different quasi-isotropic laminate plates,  $[90/\pm 45/0]_s$  and  $[90/\pm 30]_s$ , were fabricated by following the same hand-lay-up process presented earlier. The laminates containing either 2.5 or 5 wt% organoclay loading were tested, and the results were compared to the ones not including any organoclay. It is noted that for the  $[90/\pm 45/0]_s$ , there are  $0^\circ$  plies enclosed in the laminates; thus, the failure may be dominated by the fiber properties. However, from previous investigations, it appears that the influences of the organoclay are significant when the associated properties are controlled by the matrix. Thus, to diminish the fiber effect, two other laminate samples,  $[60/15/-75/-30]_s$  and  $[67.5/22.5/-67.5/-22.5]_s$ , were cut from the  $[90/\pm 45/0]_s$  laminate plate using a diamond saw with appropriate orientations. The strengths of the laminates were then evaluated from the tensile tests, and the results compared to the conventional composites are shown in Figures 14 and 15. It can be seen that, for the laminates with organoclay included, the tensile failure stresses are a little higher than those of the conventional composite laminates, although the differences are still within the statistical errors. Figures 16 and 17 demonstrate the failure specimens of  $[67.5/22.5/-67.5/-22.5]_s$  and  $[90/\pm 30]_s$  glass/epoxy nanocomposites, respectively. The areas circled with dashed lines illustrate clear fiber breakage on the failure surfaces. Unlike the  $[\pm 45]_s$  laminates, the adjacent ply constrain in the quasi-isotropic laminates is relatively appreciable such that the off-axis fiber rupture may take place when the laminates are subjected to axial loading. Apparently, the failure mechanism in the quasi-isotropic laminates is dominated by fiber breakage; thus, the effect

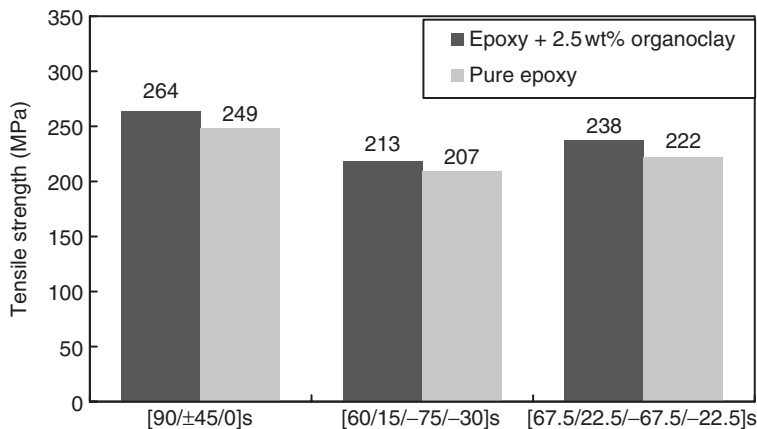


Figure 14. Organoclay effect on tensile strength of [90/±45/0]<sub>s</sub>, [60/15/-75/-30]<sub>s</sub> and [67.5/22.5/-67.5/-22.5]<sub>s</sub> glass/epoxy nanocomposite laminates.

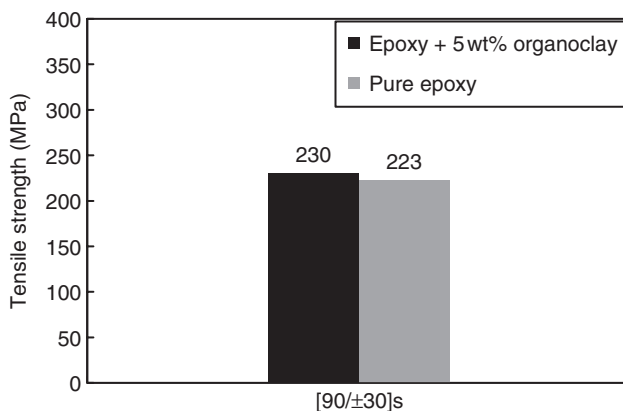
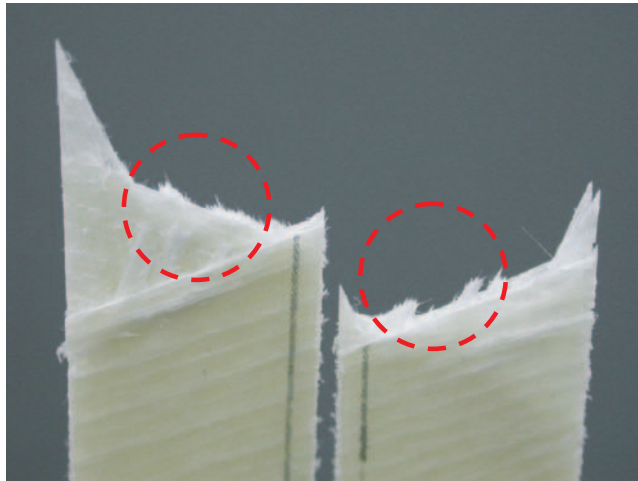


Figure 15. Organoclay effect on tensile strength of [90/±30]<sub>s</sub> glass/epoxy nanocomposite laminates.

of the organoclay on the tensile strengths of the laminates may not be as substantial as that in [±45]<sub>s</sub> laminates.

### CONCLUSIONS

The tensile, flexural and fracture behaviors of the fiber nanocomposites with different organoclay loadings were investigated experimentally. From the tensile tests, it was found that the longitudinal tensile strength of the nanocomposites slightly decreases with the increase of organoclay loadings. However, the transverse tensile strength and modulus increase as the organoclay loading increases. The enhancing behaviors could be due to the improved interfacial bonding between the fibers and surrounding matrix modified by the organoclay. Moreover, according to the tensile tests on [10]<sub>s</sub> and [±45]<sub>s</sub> specimens as well



**Figure 16.** Failure specimens of  $[67.5/22.5]_s$  glass/epoxy nanocomposite laminates with 2.5 wt% organoclay loadings.

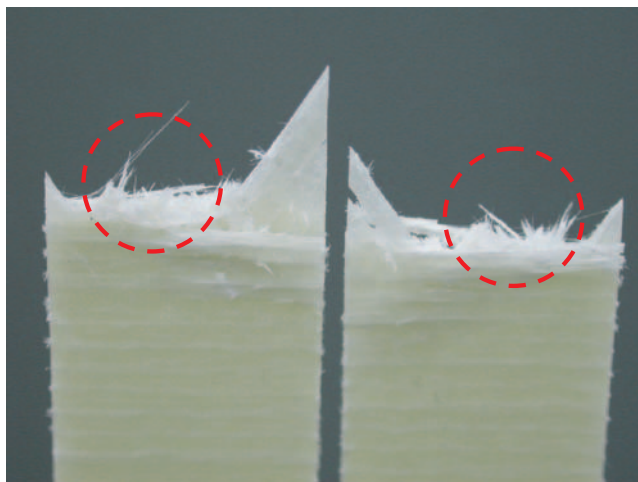


**Figure 17.** Failure specimens of  $[90/\pm 30]_s$  glass/epoxy nanocomposite laminates with 5 wt% organoclay loadings.

as the transverse flexural tests, the organoclay also exhibits a positive effect on the in-plane shear strength and the transverse flexural strength of the nanocomposites. Nevertheless, the interlaminar fracture tests indicate that the interlaminar fracture toughness of the nanocomposites decreases with the inclusion of the organoclay. The declining phenomena could be attributed to the toughened matrix caused by the presence of the organoclay. In addition, from the tensile responses of the quasi-isotropic laminates, it was found that the fiber rupture is the main failure model; thus the influence of the organoclay on the failure stress is not significant.

## ACKNOWLEDGMENTS

This research was supported by the National Science Council, Taiwan, under the contract No. NSC 94-2212-E-009-017 to National Chiao Tung University.

## REFERENCES

1. Thostenson, E.T., Li, C. and Chou, T.W. (2005). Nanocomposites in Context, *Composites Science and Technology*, **65**(3–4): 491–516.
2. Pinnavaia, T.J. and Beall, G.W. (2001). *Polymer–Clay Nanocomposites*, John Wiley & Sons, New York.
3. Usuki, A., Kawasumi, M., Kojima, Y., Okada, A., Kurauchi, T. and Kamigaito, O. (1993). Swelling Behavior of Montmorillonite Cation Exchanged for  $\omega$ -Amino Acids by  $\epsilon$ -Caprolactam, *Journal of Materials Research*, **8**(5): 1174–1178.
4. Usuki, A., Kojima, Y., Kawasumi, M., Okada, A., Fukushima, Y., Kurauchi, T. and Kamigaito, O. (1993). Synthesis of Nylon 6-Clay Hybrid, *Journal of Materials Research*, **8**(5): 1179–1184.
5. Cho, J.W. and Paul, D.R. (2001). Nylon 6 Nanocomposites by Melt Compounding, *Polymer*, **42**(3): 1083–1094.
6. Chin, I., Thurn-Albrecht, T., Kim, H., Russell, T.P. and Wang, J. (2001). On Exfoliation of Montmorillonite in Epoxy, *Polymer*, **42**(13): 5947–5952.
7. Ratna, D., Manoj, N.R., Varley, R., Raman, R.K.S. and Simon, G.P. (2003). Clay-Reinforced Epoxy Nanocomposites, *Polymer International*, **52**(9): 1403–1407.
8. Yano, K., Usuki, A., Okada, A., Kurauchi, T. and Kamigaito, O. (1993). Synthesis and Properties of Polyimide–Clay Hybrid, *Journal of Polymer Science, Part A: Polymer Chemistry*, **31**(10): 2493–2498.
9. Dennis, H.R., Hunter, D.L., Chang, D., Kim, S., White, J.L., Cho, J.W. and Paul, D.R. (2001). Effect of Melt Processing Conditions on the Extent of Exfoliation in Organoclay-Based Nanocomposites, *Polymer*, **42**(23): 9513–9522.
10. Okada, A. and Usuki, A. (1995). The Chemistry of Polymer–Clay Hybrids, *Materials Science and Engineering: C*, **3**(2): 109–115.
11. Haque, A., Shamsuzzoha, M., Hussain, F. and Dean, D. (2003). S2-Glass/Epoxy Polymer Nanocomposites: Manufacturing, Structures, Thermal and Mechanical Properties, *Journal of Composite Materials*, **37**(20): 1821–1837.
12. Kornmann, X., Rees, M., Thomann, Y., Nicola, A., Barbezat, M. and Thomann, R. (2005). Epoxy-Layered Silicate Nanocomposites as Matrix in Glass Fibre-Reinforced Composites, *Composites Science and Technology*, **65**(14): 2259–2268.
13. Chowdhury, F.H., Hosur, M.V. and Jeelani, S. (2006). Studies on the Flexural and Thermomechanical Properties of Woven Carbon/Nanoclay-Epoxy Laminates, *Materials Science & Engineering A: Structure Materials*, **421**(1–2): 298–306.
14. Miyagawa, H., Jurek, R.J., Mohanty, A.K., Misra, M. and Drzal, L.T. (2006). Biobased Epoxy/Clay Nanocomposites as a New Matrix for CFRP, *Composites Part A: Applied Science and Manufacturing*, **37**(1): 54–62.
15. Vlasveld, D.P.N., Parlevliet, P.P., Bersee, H.E.N. and Picken, S.J. (2005). Fibre-Matrix Adhesion in Glass-Fibre Reinforced Polyamide-6 Silicate Nanocomposites, *Composites Part A: Applied Science and Manufacturing*, **36**(1): 1–11.
16. Technical data sheet, Nanocor Inc.
17. Tsai, J. and Hsu, S. (2006). Organoclay Effect on Fracture Behaviors of Epoxy Nanocomposites, submitted for publication in *Journal of Materials Science*.
18. Adams, D.F., Carlsson, L.A. and Pipes, R.B. (2003). *Experimental Characterization of Advanced Composite Materials*, **3rd edn**, CRC Press, New York.



19. ASTM Standard D790-02 (2002). Standard Test Methods for Flexural Properties of Un-reinforced and Reinforced Plastics and Electrical Insulating Materials, *American Society for Testing and Materials*, West Conshohocken, PA.
20. ASTM Standard D5528-01 (2001). Standard Test Method for Mode I Interlaminar Fracture Toughness of Unidirectional Fiber-Reinforced Polymer Matrix Composites, *American Society for Testing and Materials*, West Conshohocken, PA.
21. Hashemi, S., Kinloch, A.J. and Williams, J.G. (1989). Corrections Needed in Double-Cantilever Beam Tests for Assessing the Interlaminar Failure of Fibre-Composites, *Journal of Materials Science Letters*, **8**(2): 125–129.